IRS-2 Deficiency Impairs NMDA Receptor-Dependent Long-term Potentiation

Cerebral Cortex August 2012;22:1717–1727
doi:10.1093/cercor/bhr216
Advance Access publication September 27, 2011

IRS-2 Deficiency Impairs NMDA Receptor-Dependent Long-term Potentiation

Eduardo D. Martín[1], Ana Sánchez-Perez[2,6], José Luis Trejo[3], Juan Antonio Martin-Aldana[2], Marife Cano Jaimez[2], Sebastián Pons[4], Carlos Acosta Umanzor[2], Lorena Menes[2], Morris F. White[5] and Deborah J. Burks[2]

[1]Laboratory of Neurophysiology and Synaptic Plasticity, Albacete Science and Technology Park (PCYTA), Institute for Research in Neurological Disabilities (IDINE), University of Castilla-La Mancha, 02071 Albacete, Spain, [2]Regenerative Medicine Program, Centro de Investigación Príncipe Felipe, CIBER de Diabetes y Enfermedades Metabolicas Asociadas (CIBERDEM), 46012 Valencia, Spain, [3]Cajal Institute, Consejo Superior de Investigaciones Científicas, 28002 Madrid, Spain, [4]Institute for Biomedical Research of Barcelona, IIBB-CSIC-IDIBAPS, 08036 Barcelona, Spain and, [5]Howard Hughes Medical Institute, Division of Endocrinology, Children's Hospital Boston, Harvard Medical School, Boston, MA 02115, USA and [6]Current address: Department of Physiology, University of Valencia, 46010 Valencia, Spain

Address correspondence to Deborah Burks, Regenerative Medicine Program, Centro de Investigación Príncipe Felipe, CIBER de Diabetes y Enfermedades Metabolicas Asociadas (CIBERDEM), Avenida del Autopista del Saler 16, 46012 Valencia, Spain. Email: dburks@cipf.es.

The beneficial effects of insulin and insulin-like growth factor I on cognition have been documented in humans and animal models. Conversely, obesity, hyperinsulinemia, and diabetes increase the risk for neurodegenerative disorders including Alzheimer's disease (AD). However, the mechanisms by which insulin regulates synaptic plasticity are not well understood. Here, we report that complete disruption of insulin receptor substrate 2 (Irs2) in mice impairs long-term potentiation (LTP) of synaptic transmission in the hippocampus. Basal synaptic transmission and paired-pulse facilitation were similar between the 2 groups of mice. Induction of LTP by high-frequency conditioning tetanus did not activate postsynaptic *N*-methyl-D-aspartate (NMDA) receptors in hippocampus slices from $Irs2^{-/-}$ mice, although the expression of NR2A, NR2B, and PSD95 was equivalent to wild-type controls. Activation of Fyn, AKT, and MAPK in response to tetanus stimulation was defective in $Irs2^{-/-}$ mice. Interestingly, IRS2 was phosphorylated during induction of LTP in control mice, revealing a potential new component of the signaling machinery which modulates synaptic plasticity. Given that IRS2 expression is diminished in Type 2 diabetics as well as in AD patients, these data may reveal an explanation for the prevalence of cognitive decline in humans with metabolic disorders by providing a mechanistic link between insulin resistance and impaired synaptic transmission.

Keywords: diabetes, insulin receptor signaling, long-term potentiation, NMDA receptor, synaptic plasticity

Introduction

Memory deficits that develop during the course of Alzheimer's disease (AD) have been linked to abnormalities in circulating insulin levels and/or defects in insulin signaling pathways (Luchsinger et al. 2004; Rivera et al. 2005; Craft 2007). Consistent with this, administration of insulin improves cognitive function in these patients (Kern et al. 2001; Reger et al. 2008). Evidence obtained from epidemiological studies and animal models suggest that diabetes and other metabolic disorders increase the risk for development of neurodegenerative disorders (Kuusisto et al. 1997; Vanhanen et al. 2006; Ronnemaa et al. 2008). Additionally, obesity in middle age predisposes for impaired cognitive function in the elderly (Elias et al. 2003; Whitmer et al. 2005).

Despite the accumulation of evidence to support a physiological as well as pathological role for insulin in the hippocampus, the molecular mechanisms by which this hormone modulates synaptic plasticity and memory formation remain poorly defined. Systemic insulin enters the brain through a receptor-mediated saturable transport (Baura et al. 1993). Serum insulin-like growth factor I (IGF-I) also crosses the blood-brain barrier by a transport mechanism which is regulated directly by neuronal activity; electrical, sensory, or behavioral stimulation of neurons can increase IGF-I in activated regions (Nishijima et al. 2010). IGF-I itself has been detected in astrocytes and neurons of the central nervous system (CNS) (Garcia-Segura et al. 1991; Garcia-Estrada et al. 1992). The receptors for insulin (IR) and IGF-I (IGFIR) as well as other components of these signaling pathways are expressed throughout the mammalian brain with particularly high concentrations in the hypothalamus, the hippocampus, and the cerebral cortex (Raizada et al. 1988; Unger et al. 1989; Pons 1991 #392).

The cellular effects of insulin and IGF-I are mediated principally by the insulin receptor substrate (IRS) proteins (Sun et al. 1991). Upon phosphorylation by activated hormone receptors, IRS proteins recruit various signaling molecules including phosphoinositide-3-kinase (PI3K), Fyn kinase, and Grb2 (Sun et al. 1991). The deletion of *Irs1* in mice reduces body size (Araki et al. 1994) and increases lifespan (Selman et al. 2008), whereas complete disruption of *Irs2* causes diabetes due to insulin resistance and pancreatic β cell failure (Withers et al. 1999; Burks et al. 2000). IRS1, 2, and 4 are expressed in neurons and glia throughout the CNS including cerebral cortex, hippocampus, and hypothalamic nuclei, where they can be colocalized with the IR or IGFIR (Folli et al. 1994; Ye et al. 2002).

Learning in rodents alters the expression and phosphorylation of IR in the CA1 region of the hippocampus (Zhao et al. 1999; Dou et al. 2005). In contrast, experimental diabetes in animal models is associated with defects of synaptic transmission (Yamato et al. 2004; Artola et al. 2005; Kamal et al. 2006). Once in the CNS, insulin modulates components of synaptic plasticity including recruitment of postsynaptic γ-aminobutyric acid (GABA) receptors (Wan et al. 1997; Vetiska et al. 2007), endocytosis of α-amino-3-hydroxy-5-methyl-4-isoxazolepropionic acid (AMPA) receptors (Beattie et al. 2000; Lin et al. 2000), and *N*-methyl-D-aspartate receptor (NMDAR) trafficking and function (Liu et al. 1995; Skeberdis et al. 2001; van der Heide et al. 2005). Recently, the IR has also been implicated in the regulation of synapse density within the Xenopus retina (Chiu et al. 2008).

One major obstacle to elucidating the precise role of insulin in cognition has been the lack of appropriate animal models; the majority of published studies have relied on the induction of diabetes in rodents by treatment with streptozocin, an antineoplastic agent which inhibits DNA synthesis and is associated with deleterious side effects including neurotoxicty (Rivera and Ajani 1998; Imaeda et al. 2002). With the present study, we have tested whether the insulin-resistant state induced by complete deletion of *Irs2* in mice alters the molecular events of synaptic transmission. Here, we provide evidence that *Irs2* deficiency impairs tetanus-induced long-term potentiation (LTP) in the Schaffer collateral–CA1 region.

Materials and Methods

Animals

The generation and routine genotyping of Irs2-deficient mice have been described previously (Withers et al 1998). Mice used for the present studies were maintained on a C57Bl/6 background. All experiments were performed in compliance with national regulations regarding animal welfare and were approved by the institutional committee for ethics and animal use. For routine measurements of glucose and insulin, mice were fasted for 16 h, and a small quantity of blood was obtained from the tail vein. Glucose levels were determined by glucometer (Bayer Elite). Insulin was measured by enzyme-linked immunosorbent assay (Mercodia, Sweden).

Histology

Brains were fixed in 4% paraformaldehyde. Following embedding in paraffin, serial sections of 5 microns were prepared. Subsequently, sections were deparaffinized and stained using a standard Nissl protocol.

Electrophysiology

Transverse brain slices (400 μm thickness) were prepared from female mice (3 months old) as described previously (Martin and Buno 2003) and incubated for 1 h at room temperature (21–24 °C) in ACSF infused with 95% O_2 and 5% CO_2. The artifical cerebral spinal fluid (ACSF) contained (in mM): NaCl 124, KCl 2.69, KH_2PO_4 1.25, $MgSO_4$ 2, $NaHCO_3$ 26, $CaCl_2$ 2 and glucose 10. Prior to use, ACSF was equilibrated with 95% O_2 and 5% CO_2. Slices were transferred to an immersion recording chamber and perfused (2.5 mL/min) with ACSF. Extracellular field excitatory postsynaptic potentials (fEPSPs) were recorded with a glass microelectrode (impedances: 2–3 MΩ; filled with 1 M NaCl) positioned in stratum radiatum area CA1. Evoked fEPSPs were elicited by stimulation of the Schaeffer collateral fibers with an extracellular bipolar nichrome electrode via a 2100 isolated pulse stimulator (A-M Systems, Inc., Carlsborg, WA). The stimulation intensity was adjusted to give fEPSP amplitude that was approximately 50% of maximal fEPSP sizes. LTP was induced by applying 4 trains (1 s at 100 Hz) spaced 20 s, and potentiation was measured for 1 h after LTP induction at 0.1 Hz. The responses to paired-pulse stimulation at different interpulse intervals (25–400 ms) were used to measure paired-pulse facilitation (PPF). The mean slope of the fEPSP during the first 2 min after the LTP-inducing tetanus was used to measure post-tetanic potentiation (PTP). For each experiment, fEPSP slopes were expressed as a percentage of average pretetanus baseline slope values. To measure the contribution of NMDA and AMPA receptors to fEPSP, the experiments were performed in the presence of 50 μM bicuculline to isolate EPSP from $GABA_A$-mediated inhibitory synaptic transmission. Under these conditions, 6-cyano-7-nitroquinoxaline-2, 3-dione (CNQX; 20 μM) in Mg^{2+}-free external solution (Hestrin et al. 1990) or D (–)-2-amino-5-phosphonopentanoic acid (AP5; 50 μM) was added to pharmacologically isolate both NMDA and AMPA field excitatory postsynaptic current (fEPSC) components, respectively. Train stimuli at 100 Hz were used to assess synaptic activation of the AMPA and NMDA receptors by high-frequency afferent stimulation.

Whole-cell recordings from CA1 hippocampal pyramidal neurons were made using the "blind" patch-clamp technique as previously described (Martin and Buno 2003). Patch electrodes had a resistance of 4–6 MΩ when filled with the internal solution that contained (in mM) the following: cesium gluconate 107.5, 4-(2-hydroxyethyl)-1-piperazineethanesulfonic acid (HEPES) 20, ethyleneglycol-bis(2-aminoethylether)-*N,N,N′,N′*-tetra acetic acid (EGTA) 0.2, NaCl 8, TEACl 10, Mg-ATP 4, and GTP 0.3 at pH 7.3 (adjusted with CsOH), with osmolarities between 280 and 290 mOsm/L. Whole-cell recordings in the voltage-clamp modes were obtained with an 2400 patch amplifier (A-M Systems). Fast and slow capacitances were neutralized; series resistance was compensated (≅80%), and membrane potential (Vm) was held at –60 mV. Data were discarded if the series resistance changed by more than 20% during an experiment. Evoked EPSCs were elicited by stimulation of Schaeffer collateral fibers as described previously for the fEPSPs recording. Data were filtered at 2 KHz and transferred to the hard disk of a Pentium-based computer using a DigiData 1440A interface and the pCLAMP 10.0 software (Axon Instruments, Molecular Devices Corporation, Sunnyvale, CA). For whole-cell recordings, LTP was induced either by tetanic stimulation in current clamp mode or pairing postsynaptic depolarization to 0 mV with stimulation of presynaptic Schaeffer collateral fibers at 2 Hz during 60 s (Martin and Buno 2003). To isolate EPSCs from $GABA_A$-mediated inhibitory synaptic transmission, experiments were performed in the presence of 50 μM bicuculline. With these conditions, we isolated AMPA and NMDA EPSC components using an experimental approach based on differential voltage dependence and kinetics (Collingridge et al. 1983; Hestrin et al. 1990; Martin and Pozo 2004). Indeed, when EPSCs are recorded in the presence of extracellular Mg^{2+}, the AMPA and NMDA EPSC can be isolated because at –60 mV, only the fast AMPA EPSC is recorded due to the voltage-dependent block of the NMDA receptor channel by extracellular Mg^{2+}, while at +60 mV, the slower NMDA receptor-mediated EPSC is present due to the Mg^{2+} block relief of the NMDA receptor channels (Collingridge et al. 1983; Hestrin et al. 1990; Martin and Pozo 2004). At +60 mV and at delays >50 ms, the AMPA EPSC has completely disappeared, whereas the slower NMDA EPSC is peaking and its amplitude can be estimated in isolation (Hestrin et al. 1990; Martin and Pozo 2004). All drugs were purchased from Sigma (St Louis, MO) except CNQX, AP5, and bicuculline that were from Tocris Cookson (Bristol, UK). Statistical differences were established using the 2-tailed Student's *t*-test.

Immunoprecipitation and Western Blotting

Hippocampus slices were prepared for electrophysiology as described above. Prior to the induction of LTP, slices were collected and processed as nonstimulated controls. Following the induction of LTP, hippocampal slices were collected at 5 and 30 min and frozen immediately in liquid N_2. Tissue was lysed in RIPA buffer by polytron, and homogenates were clarified by centrifugation at 12 000 × *g* for 10 min. Protein determination was by the Bradford assay. Immunoprecipitations were performed using 500 μg of total protein. The immune complexes were collected on protein A-agarose or protein G-agarose beads and subjected to sodium dodecyl sulfate–polyacrylamide gel electrophoresis (SDS-PAGE). Gels were transferred to Immobilon membranes and incubated with one of the following antibodies: anti-NR2B (Upstate), anti-phosphotyrosine (Upstate), anti-p-AKT (Cell Signaling), anti-MAPK (Santa Cruz Biotechnology Inc.), anti-IR (Santa Cruz Biotechnology Inc.), anti-IGFIR (Cell Signaling). Westerns were developed by ECL (Pierce), films scanned and immunoreactive bands quantified with the Alpha Imager program.

Isolation of Postsynaptic Densities

Mice were sacrificed by cervical dislocation, and the hippocampus was dissected from each brain. The fixed angle protocol of Villasana et al. (2006) was adapted for tabletop ultracentrifuge (Beckman Coulter Optima TLX-120) using 4 hippocampi of each genotype. Briefly, hippocampi were pooled and lysed by homogenization in ice-cold buffer (320 mM sucrose, 4 mM HEPES, pH 7.3) to which a cocktail of inhibitors was added (Complete, Roche) An aliquot of the homogenate was collected for western analysis of total lysate (T) and the remainder

was centrifuged for 10 min at 1000 × *g* in Eppendorf tubes. The resulting pellet was discarded and the supernatant was centrifuged 9200 × *g* for 15 min. The pellet containing crude synaptosomes was resuspended in hypotonic lysis buffer and centrifuged for 20 min at 250 000 × *g*. The pellet containing the postsynaptic densities (PSD) was solubilized (50 mM Tris, 150 mM NaCl, 2.5 mM ethylenediaminetetraacetic acid, 2.5 mM EGTA, pH 7.4, containing protease inhibitors), and protein concentration was measured by Bradford assay. Forty micrograms of protein from the total lysate, cytosolic fraction, and PSD fraction were separated by SDS-PAGE, and western analysis was performed as described above.

Results

Basal Synaptic Transmission Is Preserved in Irs2$^{-/-}$ Mice

We first analyzed basal synaptic transmission by applying isolated stimuli of increasing intensity to the Schaffer collaterals (Fig. 1*A*). Input/output curves for extracellular fEPSP were indistinguishable between slices from Irs2$^{-/-}$ mice and wild-type (WT) controls. For a range of stimulation intensities, the slopes of Irs2$^{-/-}$ fEPSP responses were not significantly different from the fEPSP responses of WT slices ($P > 0.05$, $n = 6$ mice of each genotype, at least 3 slices per mouse, Fig. 1*B*). Likewise, measurements of the fiber volleys amplitude from Irs2$^{-/-}$ and WT slices were similar ($P > 0.05$, $n = 6$ mice of each genotype, at least 3 slices per mouse, Fig. 1*C*), and there was no difference in an input/output curve (Fig. 1*D*). We also investigated presynaptic function to exclude the possibility that the absence of IRS2 alters the probability of neurotransmitter release. PPF ratios of fEPSP slopes at interstimulus intervals ranging from 25 to 400 ms were normal in the Irs2$^{-/-}$ mice ($P > 0.05$, $n = 6$ mice of each genotype, at least 3 slices per mouse, Fig. 1*E*,*F*). Collectively, these results indicate that Irs-2 deficiency does not modify the basal synaptic transmission at the presynaptic or postsynaptic level.

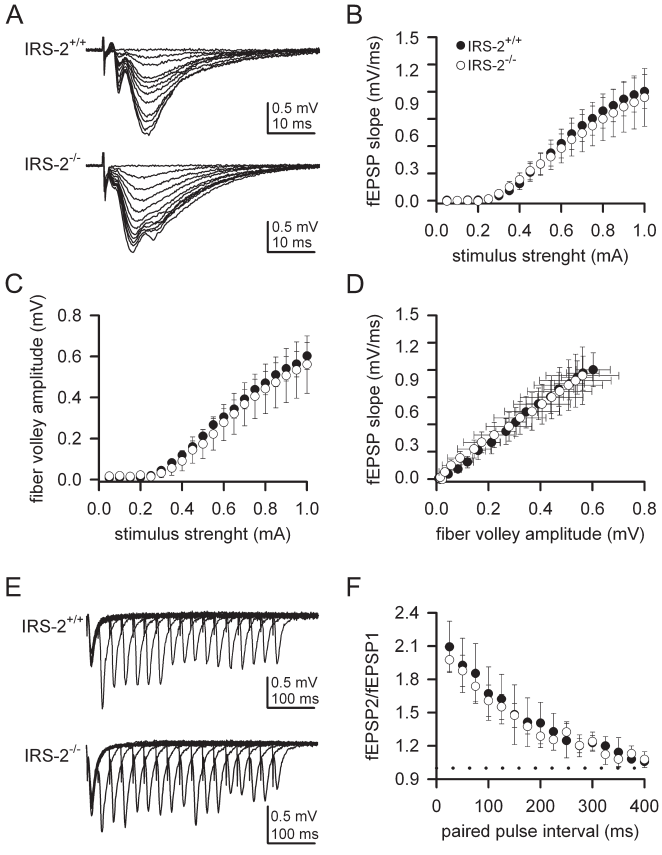

Figure 1. Basal synaptic transmission and PPF at CA1 synapses are not altered in Irs2$^{-/-}$ mice. (*A*) Representative fEPSP recorded in the stratum radiatum and evoked by stimulation of the Schaffer collateral–commissural pathway with different intensities in WT (top) and Irs2$^{-/-}$ (bottom) mice. (*B*) fEPSP slopes are comparable between Irs2$^{+/+}$ (filled circle, $n = 6$ mice) and Irs2$^{-/-}$ (open circle, $n = 6$ mice) for a given range of stimulus intensities. (*C*) Fiber volley amplitudes are similar between Irs2$^{+/+}$ (filled circle, $n = 6$) and Irs2$^{-/-}$ (open circle, $n = 6$) mice for a given range of stimulus intensities. (*D*) Input/output relationships for control (filled circle, $n = 6$) and transgenic (open circle, $n = 6$) mice. Data are presented as mean ± standard error of the mean. (*E*) Representative fEPSP recorded in stratum radiatum of slices from Irs2$^{+/+}$ (top) and Irs2$^{-/-}$ (bottom) mice at different interstimulus intervals. (*F*) PPF of fEPSPs was similar in both Irs2$^{+/+}$ ($n = 6$) and Irs2$^{-/-}$ ($n = 6$) mice. The mean slope of the paired EPSP is plotted against interpulse interval.

Loss of IRS2 Function Disables LTP at the Postsynaptic Level

Given that insulin resistance is associated with impaired neuronal function, we used the Irs2 transgenic model to assess synaptic plasticity at Schaffer collateral–CA1 synapse in the hippocampus using a high-frequency conditioning tetanus to induce LTP. LTP is the sustained increase in synaptic strength obtained after a high-frequency conditioning stimulus and is a compelling model for the synaptic mechanism underlying some forms of learning and memory (Malenka and Nicoll 1999). Baseline responses were monitored for 10–30 min before conditioning and were found to be stable. Tetanic conditioning revealed a marked difference in the ability of hippocampus slices from *Irs2*$^{-/-}$ mice to support LTP, with potentiation of fEPSP being significantly reduced in slices from transgenic animals as compared with WT ($n = 6$ mice of each genotype, at least 3 slices per mouse, $P < 0.001$, Fig. 2*A*). To evaluate whether the lack of tetanus-induced LTP might reflect insufficient cumulative depolarization during tetanic stimulation, LTP was induced by pairing postsynaptic depolarization with presynaptic stimulation via patch-clamp techniques in whole-cell recordings (see Materials and Methods). This LTP was also completely impaired in *Irs2*$^{-/-}$ mice ($n = 4$ mice of each genotype, at least 2 slices per mouse, $P < 0.001$, Fig. 2*B*), indicating that IRS2 signaling is required to maintain synaptic plasticity at Schaffer collateral–CA1 synapse in the hippocampus. To test the possibility that increased inhibition causes the impaired LTP in Irs2$^{-/-}$ mice, tetanic conditioning was applied to control and transgenic slices in the presence the $GABA_A$ receptor antagonist bicuculline (50 μM). However, under these conditions, the defective LTP persisted in Irs2$^{-/-}$ mice (Fig. 2*C*), demonstrating that increased inhibition was not responsible for the inability to induce LTP in the absence of IRS2 signals. Moreover, PTP of the fEPSP revealed no significant differences between slices from mutant and control animals (mean percent of baseline before tetanus: Irs2$^{+/+}$ 98.7 ± 1.2%, $n = 6$ mice; Irs2$^{-/-}$ 99.6 ± 0.8%, $n = 6$ mice; following tetanus: Irs2$^{+/+}$ 256.1 ± 15.4%, $n = 6$ mice; Irs2$^{-/-}$ 217.2 ± 21.1%, $n = 6$ mice). PTP is postulated to indicate presynaptic function, reflecting a period of enhanced transmitter release caused by the loading of the presynaptic terminals with calcium ions during tetanic conditioning (Zucker 1989). Therefore, these results demonstrate clearly that the impairment of LTP observed in the hippocampus of Irs2$^{-/-}$ is due to defects at the postsynaptic level without a reduction of neurotransmitter release. Moreover, the impaired LTP was not related with diabetic complications in the Irs2$^{-/-}$ animals since 8-week-old females with normal glucose and insulin levels were

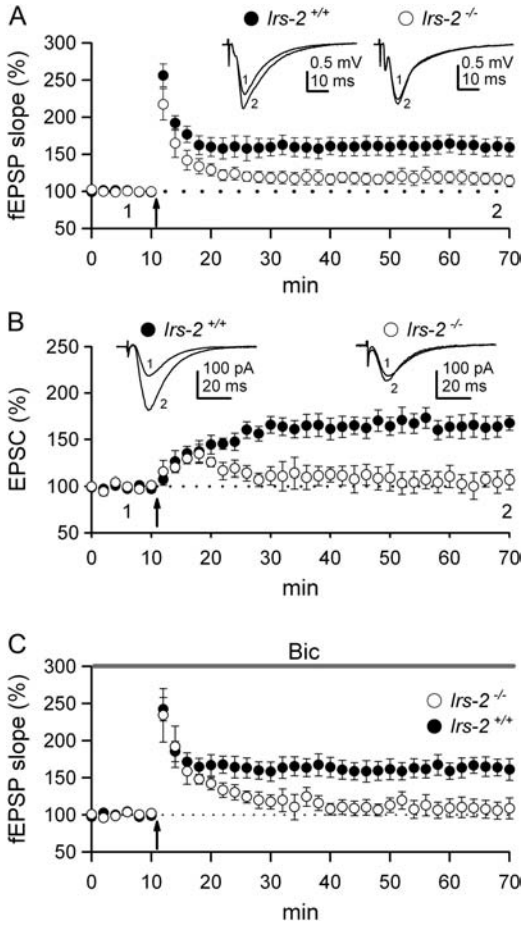

Figure 2. Synaptic plasticity at CA1 synapses is altered in the absence of IRS2 signals. (*A*) Summary of time course of mean fEPSPs slope in hippocampus slices from WT (filled circle, $n = 6$ mice) and Irs2$^{-/-}$ (open circle, $n = 6$ mice) in basal conditions and following induction of LTP. At least 2 slices from each hippocampus used. Data were normalized for each slice with respect to the average slope recorded during baseline. The insert depicts a representative superimposed recording taken before and after LTP induction in both groups of mice. (*B*) Representative EPSC averages (inset traces) and summary data of LTP induced by pairing postsynaptic depolarization during 60 s with presynaptic stimulation (2 Hz) using patch-clamp techniques, in WT (filled circle, $n = 4$ mice) and Irs2$^{-/-}$ (open circle, $n = 4$ mice). (*C*) The impaired LTP in Irs2$^{-/-}$ (filled circle, $n = 4$) mice was insensitive to the suppression of inhibition with 50 μM of the $GABA_A$ receptor antagonist bicuculline (Bic).

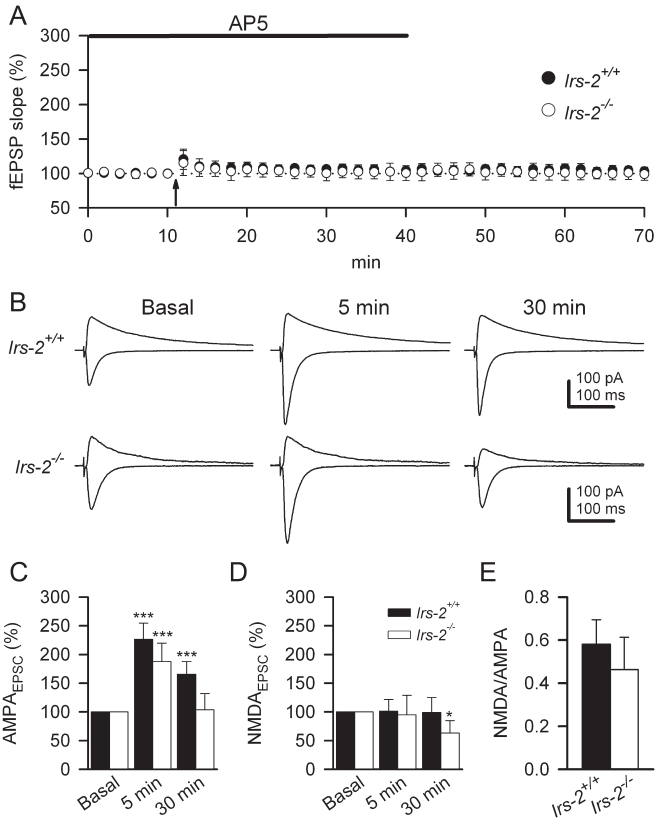

Figure 3. Relative contributions of AMPA and NMDA receptors to the impaired LTP of Irs2-deficient mice. (*A*) Expression of LTP was blocked by 50 μM AP5, an antagonist of NMDA receptors, in both WT and (filled circle, $n = 4$ mice) and Irs2$^{-/-}$ (open circle, $n = 4$ mice) hippocampus. (*B*) Representative EPSC means in WT (top traces) and Irs2$^{-/-}$ (bottom traces) slices recorded at −60 ($AMPA_{EPSCs}$) and +60 mV ($NMDA_{EPSCs}$) in basal conditions and 5 and 30 min after LTP induction. (*C*) Summary of mean $AMPA_{EPSCs}$ peak amplitudes (recorded at −60 mV) in WT (filled bar, $n = 4$) and Irs2$^{-/-}$ (open bar, $n = 4$) mice. Whereas $AMPA_{EPSCs}$ in WT slices were significantly potentiated at 30 min following LTP induction, they were reduced to basal values in Irs2$^{-/-}$ slices. (*D*) Summary graph depicting mean $NMDA_{EPSCs}$ peak amplitudes (recorded at +60 mV at 100 ms delay) in WT (filled bar, $n = 4$) and Irs2$^{-/-}$ (open bar, $n = 4$) mice. $NMDA_{EPSCs}$ in Irs2$^{-/-}$ were significantly reduced at 30 min following LTP induction. Error bars indicate standard error of the mean (SEM). Significant differences were established at $^{***}P < 0.001$. (*E*) Ratios of amplitudes of the whole-cell currents recorded at −60 and +60 mV. The NMDA receptor-dependent responses (measure at 100 ms delay) were similar in the Irs2$^{+/+}$ (filled bar) and Irs2$^{-/-}$ (open bar) slice. Error bars indicate SEM.

used for all experiments of the current study (Supplementary Fig. 1*A,B*). Deletion of Irs-2 produces diabetes in mice due to reduced beta cell mass and peripheral insulin resistance; however, the development of diabetes in this model displays a sexual dimorphism which affects males earlier and more severely than females (Burks et al. 2000). Given the critical role of IRS-2 in brain development (Schubert et al. 2003), we examined the formation of the hippocampus but found no gross morphological differences between genotypes (Supplementary Fig. 1*C*).

Irs2$^{-/-}$ Mice Display an Inadequate Synaptic Activation of NMDA Receptors

LTP in the hippocampus is expressed as an increase of the slope and amplitude of the fast component of EPSP mediated by the AMPA subtype of glutamate receptor (Schubert et al. 2003). However, it is generally agreed that induction of the classical LTP requires the activation of postsynaptic NMDA receptors (Bliss and Collingridge 1993). Consistent with this, the NMDAR antagonist AP5 completely abolished the induction of LTP in WT and Irs2$^{-/-}$ mice ($n = 4$ mice of each genotype, at least 2 slices per mouse, Fig. 3*A*), confirming that this type of LTP indeed requires NMDA receptor activation. To quantify the relative contributions of AMPA- and NMDA receptor-mediated synaptic components under our experimental conditions, patch-clamp recordings from whole cells were made during the first 30 min following tetanic stimulation under current clamp mode, using an experimental approach based on different voltage dependence and kinetics (see Materials and Methods). The AMPA receptor-mediated component of the evoked EPSC ($AMPA_{EPSC}$) measured at –60 mV increased 5 min after tetanic stimulation in WT and Irs2$^{-/-}$ samples (Fig. 3*B,C*). However, although the $AMPA_{EPSC}$ amplitude was maintained 30 min after tetanus in WT (Fig. 3*B,C*), these recordings returned

to baseline values in Irs2$^{-/-}$ animals. The amplitude of NMDAR-mediated component ($NMDA_{EPSC}$), measured at +60 mV and at delays of 100 ms, was not significantly different from baseline values at 5 and 30 min after tetanus in WT slices ($n = 4$ mice of each genotype, at least 3 slices per mouse, Fig. 3*B,D*), in agreement with previous observations (Kullmann 1994; Nicoll and Malenka 1999; Poncer and Malinow 2001). This potentiation of the $AMPA_{EPSC}$ component, without changes to the $NMDA_{EPSC}$ component, characterizes the classical LTP of Schaeffer collateral EPSCs in CA1 pyramidal neurons (Kullmann 1994; Nicoll and Malenka 1999; Poncer and Malinow 2001). However, with slices from Irs2$^{-/-}$ mice, the $NMDA_{EPSC}$ declined significantly to below baseline values 30 min after tetanus (63 ± 21%, $n = 4$ mice of each genotype, at least 3 slices per mouse, $P < 0.05$, Fig. 3*B,D*). The observed deficit of the NMDAR-mediated component of EPSC in Irs2$^{-/-}$ slices could be the result of either alterations to the number or properties of the synaptic NMDA receptors or inadequate activation of NMDA receptors during the high-frequency stimulation. To distinguish between these possibilities, we first examined the ratio of NMDAR-mediated to AMPA receptor-mediated synaptic currents, which controls for slice-to-slice variability in the number of synapses activated (Saal et al. 2003). First, the AMPA receptor-mediated synaptic current amplitude was measured at a holding potential of –60 mV. Then, recording from the same cell, the NMDAR-mediated current was recorded at a holding potential of +60 mV and its amplitude was measured at delays >50 ms (see Materials and Methods). The calculated ratio was similar between Irs2$^{-/-}$ and WT mice (Fig. 3*B,E*). We next investigated whether synaptic activation of AMPA or NMDA receptors was normal using fEPSP recordings during a stimuli train (100 Hz) where the NMDA component was isolated with CNQX in Mg^{2+}-free solution and the AMPA component with AP5 in normal ACSF (Hestrin et al. 1990; Martin and Pozo 2004). Under these conditions, the recordings for the AMPA receptor-mediated component of fEPSP were similar between WT and Irs2$^{-/-}$ slices (Fig. 4*A,B*). In contrast, we observed that the percentage of the second, third, and fourth fEPSP slope over the first fEPSP in the train of isolated NMDA component was significantly smaller in the Irs2$^{-/-}$ when compared with that of WT slices (second fEPSP: 137.5 ± 19.6% for Irs2$^{+/+}$ vs. 59.6 ± 19.5% for Irs2$^{-/-}$, $P < 0.05$; third fEPSP: 45.3 ± 15.7% for Irs2$^{+/+}$ vs. 7.2 ± 12.1% for Irs2$^{-/-}$, $P < 0.01$; 35.3 ± 11.2% for Irs2$^{+/+}$ vs. 5.7 ± 9.5% for Irs2$^{-/-}$ to fourth fEPSP, $P < 0.01$; $n = 4$ mice of each genotype, at least 3 slices per mouse, Fig. 4*C,D*). Collectively, these results demonstrate that Irs2 null mice display inadequate activation of postsynaptic NMDARs.

Tyrosine Phosphorylation of NR2B Subunit of NMDA Receptors Is Reduced in Irs2 Null Mice

We next performed a series of experiments to elucidate the contributions of NMDAR subtypes to the defect observed in Irs2 null mice. We recorded pharmacologically isolated NMDAR-mediated EPSCs by using whole-cell voltage clamp in the presence of 50 μM bicuculline and 20 μM CNQX in Mg^{2+}-free external solution. Application of ifenprodil (3 μM), an NR2B-subtype-specific antagonist, reduced the NMDAR-mediated EPSCs in WT mice (Fig. 5*A*; 51.8 ± 7%; $n = 4$ mice of each genotype, at least 2 slices per mouse). In contrast, the same treatment had only a minor effect on NMDAR-mediated EPSCs of Irs2 null mice (Fig. 5*A*; 91.9 ± 9%; $n = 4$ mice of each genotype, at least 2 slices per mouse). These results strongly suggest that NR2B-containing NMDARs play an important role in the synaptic plasticity modulated by IRS2 signaling.

Various lines of evidence indicate that the NR2B subunit of NMDA receptors undergoes tyrosine phosphorylation during

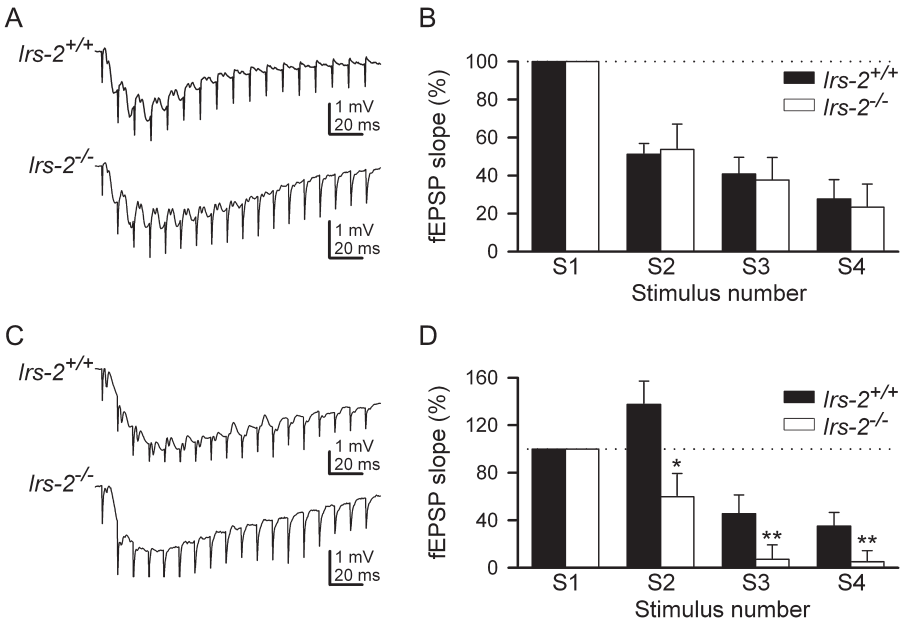

Figure 4. Inadequate activation of synaptic NMDA receptors during the high-frequency stimulation in the Irs2$^{-/-}$ transgenic mice. (*A*) Representative field responses of AMPA component evoked by a 100 Hz train during 200 ms in Irs2$^{+/+}$ (top traces) and Irs2$^{-/-}$ (bottom traces), recorded in the presence of 50 μM AP5 to block NMDA component. (*B*) Summary data showing mean AMPA isolated fEPSP slopes in Irs2$^{+/+}$ (filled bar; $n = 4$) and Irs2$^{-/-}$ (open bar; $n = 4$) mice, that were plotted against the number of the stimulus during 100 Hz train. The fEPSP slope at the 4 initial stimuli was calculated as the percentage of the first fEPSP slope. (*C*) Representative field responses of NMDA component evoked by a 100-Hz train during 200 ms in Irs2$^{+/+}$ (top tracings) and Irs2$^{-/-}$ (bottom tracings), recorded in the presence of 20 μM CNQX to block AMPA component. (*D*) Summary data showing mean NMDA isolated fEPSP slopes in IRS-2$^{+/+}$ (filled bar; $n = 4$) and IRS-2$^{-/-}$ (open bar; $n = 4$) mice. The fEPSP slope was significantly smaller in the IRS-2$^{-/-}$ for the second, third, and fourth stimuli. Significant differences were established at $^{*}P < 0.05$ and $^{**}P < 0.01$.

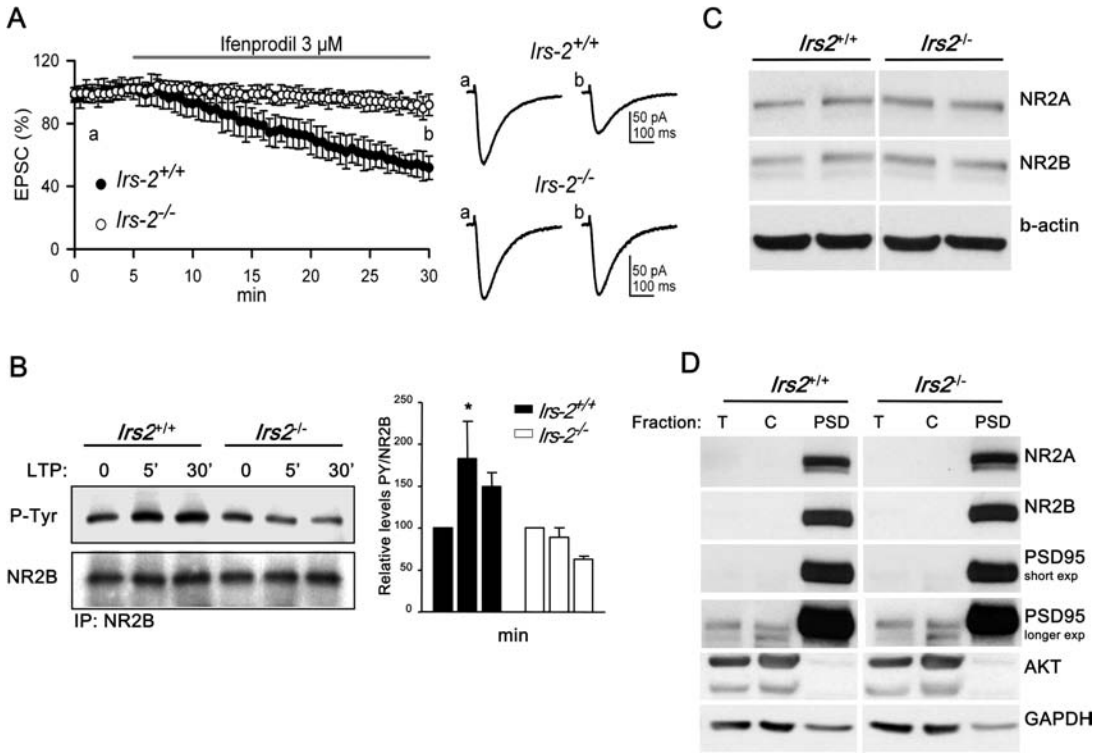

Figure 5. Irs2 deficiency impairs activation of the NR2B subunit of NMDA receptors. (*A*) Inhibition of NR2B-containing NMDAR-mediated EPSCs by ifenprodil. Plots represent normalized NMDAR-mediated EPSCs recorded by whole-cell voltage clamp (Vm = −65 mV) before and after application of ifenprodil (3 μM) as indicated. The experiment was performed in the presence of 50 μM bicuculline, 20 μM CNQX in Mg^{2+}-free external solution. Values represent mean ± standard error of the mean (n = 4 mice of each genotype, at least 2 slice per mouse). Right panel contains sample EPSC traces recorded at different time points. (*B*) Hippocampus slices were collected before (0 min) and after (5 and 30 min) induction of LTP with tetanus stimulation. Following immunoprecipitation with anti-NR2B antibodies, western blotting was performed with anti-phosphotyrosine antibodies (PY) as well as with anti-NR2B. Western blots were scanned and quantified by Alpha Imager. Tetanus stimulation did not induce tyrosine phosphorylation of NR2B in slices from $Irs2^{-/-}$ animals. Graph represents data from 3 independent experiments, with n of 9 WT and 9 $Irs2^{-/-}$ mice. (*C*) Western analysis of NMDAR expression. Fifty micrograms of individual hippocampus lysates were probed with antibodies specific for either NR2A or NR2B. Anti-β-tubulin was used to confirm equal protein loading. The images reflect a 40 s exposure of ECL detection. The results shown are representative of 2 independent experiments (WT = 4 mice; $Irs2^{-/-}$ = 4 mice). (*D*) Western analysis of subcellular fractions isolated from hippocampus. Four hippocampi of each genotype were pooled to prepare PSD as described in Materials and Methods. Forty micrograms of the indicated fractions were used for immunoblotting. T: total lysate, C: cytosol. With the exception of the image labeled "PSD95 longer exposure," the exposure time for detecting the indicated proteins by ECL was 15 s. Due to the significant enrichment of NR2A, NR2B, and PSD95 in the PSD fraction, a longer exposure (40 s) was required to detect these proteins in the total lysate as illustrated by the additional image of PSD95.

induction of LTP (Rostas et al. 1996). The NR2B contains 3 tyrosine phosphorylation sites which are targeted by Fyn (Nakazawa et al. 2001). To assess the tyrosine phosphorylation of NR2B in IRS-2 deficient mice, hippocampal slices were collected prior to induction of LTP and at 5 and 30 min after tetanic stimulation. These slices were then lysed and analyzed by western blotting. Consistent with previous reports (Rostas et al. 1996), tetanus increased significantly the tyrosine phosphorylation of NR2B after 5 min in WT slices (Fig. 5*B*), and this activation persisted until 30 min. However, in hippocampus slices from $Irs2^{-/-}$ mice, tetanus stimulation did not produce tyrosine phosphorylation of NR2B at either of the time points (Fig. 5*B*).

The failure to trigger tyrosine phosphorylation of NR2B with tetanus stimulation could not be attributed to reduced expression of this subunit since the levels detected by western blotting in hippocampus slices were equivalent between WT and Irs2 mutant mice (Fig. 5*B*,*C*). Given that NR2B appeared to be inactive in $Irs2^{-/-}$ mice, we assessed whether increased expression of NR2A might reflect a compensatory mechanism in this model. However, western blotting analysis of hippocampus lysates revealed that the expression of NR2A (as well as NR2B) was equivalent between both genotypes (Fig. 5*C*). Another potential explanation for the impaired function of NR2B is failed targeting to the PSD in the hippocampus of $Irs2^{-/-}$ animals. The PSD is a structural network of receptors, ion channels, and signaling proteins which are required for synaptic function (Feng and Zhang 2009). To investigate this possibility, PSD fractions were prepared from hippocampus of both experimental groups. Aliquots of total lysate, cytosol, and PSD were analyzed by western blotting. PSD95, a scaffolding protein which forms complexes with NMDAR (Sheng 2001), was used as a marker of PSD. Due to the significant enrichment of PSD95 in the PSD fraction, a longer exposure (40 vs. 15 s) was required to detect this marker as well as NR2A and NR2B in an equivalent amount of total lysate; however, using this exposure time, the ECL detection of these proteins in the PSD was saturated. Other markers which were used to assess the quality and quantity of the preparations included AKT (cytosolic fraction) and GAPDH (loading control for total lysate). Interestingly, no differences were detected between WT and $Irs2^{-/-}$ with respect to the targeting of NR2A, NR2B, or PSD95 to the PSD. Thus, these results suggest that impaired activation of NR2B in response to tetanus in hippocampus slices of Irs2 KO cannot be attributed to a general failure of the targeting of NR2B to the PSD.

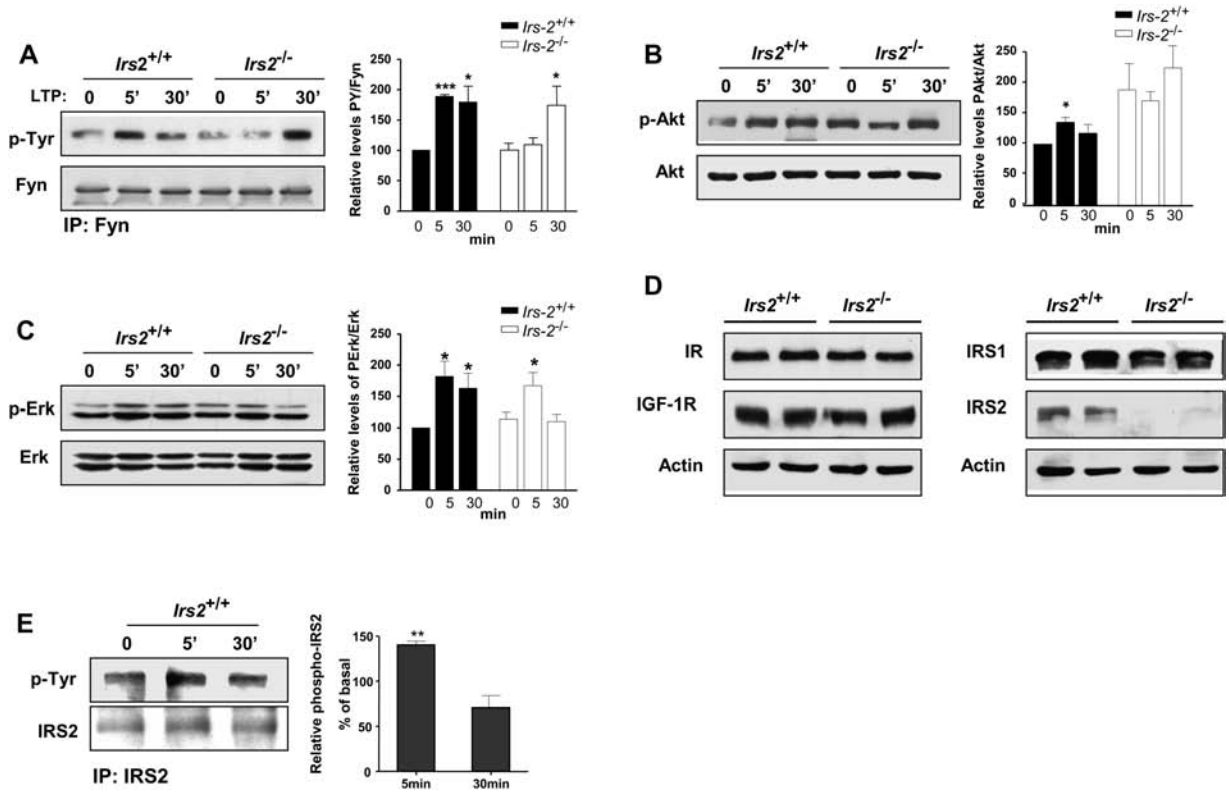

Figure 6. Failed LTP is associated with impaired signaling in hippocampus slices from Irs2$^{-/-}$ mice. (*A*) Hippocampus slices were collected before (0 min) and after (5 and 30 min) induction of LTP with tetanus stimulation. Protein lysates were prepared and immunoprecipitated with anti-Fyn antibodies. Subsequent western blotting with anti-PY revealed a significant delay in the tyrosine phosphorylation of Fyn in hippocampus slices from Irs2 null mice. Graph represents data from 3 independent experiments, $n = 9$ WT mice and 9 Irs2$^{-/-}$ mice. (*B*) Fifty micrograms of hippocampus lysates were loaded for western blotting. Induction of LTP was coincident with activation of Akt in WT but not Irs2$^{-/-}$ slices due to high basal levels phospho-Akt. Graph represents data from 5 independent experiments, $n = 15$ WT and 15 Irs2$^{-/-}$ mice. (*C*) Activation of MAPK in response to LTP induction was not sustained at 30 min in IRS-2 deficient mice. Graph represents data from 7 independent experiments, $n = 14$ WT and 12 Irs2$^{-/-}$ mice. (*D*) Fifty micrograms of hippocampus lysates were loaded for western analysis of the expression levels of the insulin receptor (IR), IGF-I receptor (IGFIR), and IRS1. No differences were noted between WT and Irs2 null mice. (*E*) Following lysis of hippocampus slices as described above, samples were immunoprecipitated for IRS2. Western blotting with anti-PY antibodies revealed that induction of LTP with tetanus stimulation induces the tyrosine phosphorylation of IRS2. Data are representative of 2 independent experiments, $n = 6$ WT and 6 Irs2 null mice.

Irs2 Deficiency Impairs Activation of Signaling Pathways Associated with LTP and Synaptic Transmission

To relate the impaired LTP to a molecular mechanism, we next examined intracellular signal transduction during the induction of LTP. Upon activation of insulin and IGF-I receptors by ligand binding, these receptor tyrosine kinases phosphorylate IRS proteins, enabling them to recruit and activate other signaling molecules (White 1997). Fyn is a nonreceptor tyrosine kinase which mediates the effects of insulin in various tissues (Davidson et al. 1994; Mastick and Saltiel 1997). Interestingly, ablation of Fyn in mice impairs LTP without alterations to basal synaptic transmission and PPF (Grant et al. 1992). Upon insulin stimulation, Fyn associates with phosphorylated tyrosine residues of IRS proteins via its src homology (SH) 2 domain (Sun et al. 1996). Therefore, we evaluated the activation of Fyn in response to tetanus stimulation in hippocampus slices from WT and Irs2-deficient mice. At 5 min poststimulus, the activation of Fyn as detected by anti-phosphotyrosine antibodies was increased significantly in WT slices (Fig. 6*A*) and persisted at 30 min, although the levels were slightly lower than at 5 min. In sharp contrast, tetanus stimulation did not induce tyrosine phosphorylation of Fyn in Irs2$^{-/-}$ slices at 5 min; however, after 30 min, the levels of tyrosine-phosphorylated Fyn were comparable to those detected in WT slices. Thus, these results suggest that IRS2 signals are required for the proper temporal phosphorylation of Fyn in response to high trains of tetanus stimulation.

Once phosphorylated on specific tyrosine residues, IRS proteins also recruit and activate PI3-K through a direct interaction with the p85 catalytic subunit (Myers et al. 1992). Interestingly, PI3K activity and its subsequent phosphorylation of Akt are also necessary for expression of LTP (Man et al. 2003; Wang et al. 2003). In our analysis of signal transduction pathways, we observed that the levels of phosphorylated Akt increased 5 min after the induction of LTP in slices from WT mice (Fig. 6*B*) and returned to basal levels after 30 min. However, in hippocampus slices from Irs2$^{-/-}$ mice, tetanus did not produce an increase of phosphorylated AKT at 5 min, perhaps owing to the fact that the basal levels of phospho-Akt were higher than in slices from WT controls (Fig. 3*B*). In peripheral tissues such as liver and muscle, Irs2-deficiency has been associated with elevated basal levels of PI3K and AKT which impairs the ability of insulin or IGF-I to activate these pathways (Withers et al. 1998).

The MAPK/ERK pathway mediates certain forms of NMDA-dependent LTP (English and Sweatt 1996; Winder et al. 1999; Kanterewicz et al. 2000; Shalin et al. 2006). Insulin can activate MAPK/ERK either directly via its receptor or by the IRS/Grb2/ras complex (Avruch 1998). Analysis of ERK phosphorylation in

hippocampus slices revealed that at 5 min poststimulus there were no differences between WT and Irs2$^{-/-}$ mice; however, after 30 min, phospho-ERK levels remained elevated in WT samples (Fig. 6*C*), whereas they returned to basal levels in Irs2$^{-/-}$ slices. Thus, these results demonstrate that IRS-2 signals are essential for sustained activation of ERK during the induction of LTP by tetanic stimulation.

The defects in these signaling pathways could not be explained by alterations to the expression of the IR, IGF-IR, or IRS-1 since the levels of these proteins in hippocampus were equivalent between WT and Irs2$^{-/-}$ mice (Fig. 6*D*). Given that the ability of IRS proteins to orchestrate intracellular signaling is dependent on their tyrosine phosphorylation, we next examined the possibility that induction of LTP by high trains of tetanus stimulation promotes the tyrosine phosphorylation of IRS2. Thus, IRS2 was immunoprecipitated from WT hippocampus slices which had been subjected to tetanus stimulation, and the immune complexes were analyzed subsequently by western blotting using anti-phosphotyrosine antibodies. Interestingly, the tyrosine phosphorylation of IRS2 was increased significantly at 5 min poststimulus but returned to basal levels after 30 min (Fig. 6*E*). Collectively, these results are consistent with a role for IRS2 in recruiting and activating other signaling pathways implicated in the expression of LTP including Fyn kinase and Akt.

Discussion

Previous studies have demonstrated that IRS2 is required for neuronal development (Schubert et al. 2003) and for CNS-mediated regulation of appetite (Burks et al. 2000). Whole-body deletion of Irs2 causes insulin resistance by disabling insulin signaling pathways; Irs2-deficiency causes hyperphagia and obesity due to impaired insulin signaling in specific populations of hypothalamic neurons (Kubota et al. 2004; Choudhury et al. 2005). In the present study, we have identified IRS2 as a novel component of the signaling apparatus which mediates synaptic plasticity in the hippocampus. Through a series of electrophysiological studies, we have demonstrated that expression of LTP is significantly impaired in *Irs2* null mice. This impairment of LTP occurs at the postsynaptic level without a reduction to neurotransmitter release since we did not detect significant differences in paired-pulse facilitation, synaptic fatigue, or PTP between WT and Irs2$^{-/-}$ mice.

Several observations from our study demonstrate that IRS2 signals may participate in the activation of postsynaptic NMDA receptors during high-frequency stimulation. First, Irs2$^{-/-}$ mice did not present alterations to the number or properties of the synaptic NMDARs. Second, when we isolated specifically the $NMDA_{EPSC}$ component of LTP, we observed a significant decline to below baseline values 30 min after tetanus in IRS-2$^{-/-}$ mice, while no changes were noted in WT control animals. Finally, the fEPSPs slopes of the isolated NMDA component in a 100 Hz train (the frequency that induces LTP under our experimental conditions) were significantly smaller in the Irs2$^{-/-}$ slices when compared with those registered in control slices. Importantly, the ratio of NMDA/AMPA synaptic currents, which controls for slice-to-slice variability in the number of synapses activated (Saal et al. 2003), was similar between Irs2$^{-/-}$ and control mice. Modulation of synaptic transmission appears to be a specific role for IRS-2 since mice deficient for IRS1, 3, or 4 have no reported CNS defects (Araki et al. 1994; Liu et al. 1999).

The present observation that IRS2 signals participate directly in LTP raises questions about precisely how this docking molecule modulates synaptic plasticity. Our analysis of the signaling pathways during induction of LTP in hippocampus slices has revealed that the absence of IRS2 impairs tyrosine phosphorylation of NR2B and activation of Fyn kinase, AKT, and MAPK in hippocampal slices. Interestingly, insulin and IGF-I regulate these pathways by SH2 domains (Schlessinger et al. 1992). By employing IRS proteins to engage other signaling molecules, the IR circumvents stoichiometric constraints encountered by receptors that directly recruit SH2 proteins to their autophosphorylation sites; one IRS molecule can simultaneously bind various SH2-containing molecules (e.g., Fyn, p85 PI3K, and Grb2). Given that IRS proteins are not tethered to the plasma membrane, the recruitment of these molecules to IRS2 may serve the critical function of relocalizing activated signaling pathways to a site within the neuron where they can modulate synaptic plasticity.

Mice deficient for Fyn kinase display impaired LTP and deficits of spatial learning (Grant et al. 1992). However, no studies to date have addressed the upstream signals that activate Fyn during the induction of LTP. We observed that Fyn was fully phosphorylated 5 min after the application of tetanus trains in normal mice, whereas this did not occur until 30 min in hippocampus slices from Irs2$^{-/-}$ mice. Given that Fyn is activated upon the interaction of its SH2 domain with phosphorylated IRS proteins (Sun et al. 1996), our findings suggest that IRS2 plays an important role in regulating the activity of this kinase. Thus, when IRS2 signals are absent or reduced, the delayed postsynaptic activation of Fyn may impair the ability of this kinase to phosphorylate the NR2B subunits of NMDA receptors, an event which potentiates NMDA channel activity (Yu et al. 1997; Xu et al. 2006). Our studies demonstrate that that the expression of NR2A and NR2B as well as their targeting to PSDs is preserved in Irs2-deficient mice, excluding these potential alterations as explanations for the impaired LTP.

Irs2 deficiency has been shown previously to impair the activation of PI3K/AKT in liver and muscle of Irs2$^{-/-}$ mice (Withers et al. 1998). PI3K has been linked to the insertion of AMPA receptors at activated CA1 synapses (Man et al. 2003) and to the inhibition of GSK3β activity during the induction of LTP (Peineau et al. 2007), whereas AKT activity is required for the cell surface expression of GABA receptors (Wang et al. 2003). Hence, our observation that conditioning tetanus is unable to activate AKT in hippocampus slices of Irs2-deficient mice suggests that IRS2 serves as an important upstream element for the regulation of synaptic PI3K/AKT signaling.

Surprisingly, induction of LTP in WT hippocampus slices increased tyrosine phosphorylation of IRS2. Given that IRS proteins are phosphorylated exclusively by receptors for insulin and IGF-I, this observation requires further study to determine precisely how IRS2 becomes activated during application of conditioning tetanus to hippocampus slices. Depolarization of rat neuronal cultures by potassium ions has been reported to stimulate a significant release of insulin (Clarke et al. 1986). Therefore, it is possible that induction of LTP in the Schaeffer collateral fibers by tetanus trains causes neurons and/or astrocytes to release insulin and/or IGF-I into their surroundings and this, in turn, induces the phosphorylation of IRS2 via the activation of postsynaptic insulin receptors. Alternatively, physiological levels of systemic insulin may modulate synaptic plasticity in vivo by promoting the

phosphorylation of IRS2 within neurons that are receptive to LTP. Whole-body deletion of Irs2 causes insulin resistance and other metabolic abnormalities by disabling insulin signaling pathways; Irs2-deficient mice eat more than control mice due the presence of insulin resistance in specific populations of hypothalamic neurons (Burks et al. 2000; Kubota et al. 2004; Chodbury et al 2005). Similarly, failed LTP in the hippocampus of Irs2 null mice may also reflect a form of insulin resistance which undermines the proper activation of AKT and Fyn in the PSD.

Studies of human subjects as well as experimental animal models demonstrate that diabetes adversely affects learning and memory (Biessels et al. 1996; Desrocher and Rovet 2004; Messier 2005; Stranahan et al. 2008). Our present results suggest that IRS2 expression and/or function may represent an important link between metabolic disorders and synaptic plasticity. Irs2 expression is significantly reduced in pancreatic islets from humans with Type 2 diabetes (Gunton et al. 2005), consistent with a critical role for IRS2 in maintaining normal sensitivity to insulin. Interestingly, reduced expression and/or function of insulin and IGF-I signaling molecules have been detected in AD brains (Craft 2007; Moloney et al. 2008). By establishing a molecular connection between systemic insulin/IGF-I resistance and impaired synaptic transmission, our observations suggest that lifestyle changes or pharmacological agents that target the expression and/or function of IRS2 may prevent neuronal dysfunction in patients with metabolic diseases.

Supplementary Material

Supplementary material can be found at: http://www.cercor.oxfordjournals.org/

Funding

This research was funded, in part, by the following grants: SAF2008-00011 (to D.J.B.), BFU2007-60195 (to J.L.T.), BFU2008-04196 (to E.D.M.), Ministerio de Ciencia e Innovación; CIBER de la Diabetes y Enfermedades Metabólicas (to D.J.B.), Instituto de Salud Carlos III; PAI07-0042-1097 and PEII10-0095-872 (to E.D.M.) from Consejería de Educación Ciencia y Cultura of the Junta Cultural de Castilla-La Mancha (JCCM), PI-2007/49 (to E.D.M.) from Fundación para la investigación sanitaria de Castilla-La Mancha; EMER-07/012 (to D.J.B.), Instituto de Salud Carlos III; Regenerative Medicine Program of Valencia (to D.J.B.); and the INCRECyT project (to E.D.M.) from European Social Fund and JCCM.

Notes

We would like to acknowledge Alberto Hernandez Cano and Eva Lafuente Villarreal of the CIPF Confocal Microscope Service for their technical assistance. *Conflict of Interest* : None declared.

References

Araki E, Lipes MA, Patti ME, Bruning JC, Haag B, Johnson RS, Kahn CR. 1994. Alternative pathway of insulin signalling in mice with targeted disruption of the IRS-1 gene. Nature. 372:186–190.

Artola A, Kamal A, Ramakers GM, Biessels GJ, Gispen WH. 2005. Diabetes mellitus concomitantly facilitates the induction of long-term depression and inhibits that of long-term potentiation in hippocampus. Eur J Neurosci. 22:169–178.

Avruch J. 1998. Insulin signal transduction through protein kinase cascades. Mol Cell Biochem. 182:31–48.

Baura GD, Foster DM, Porte D, Jr., Kahn SE, Bergman RN, Cobelli C, Schwartz MW. 1993. Saturable transport of insulin from plasma into the central nervous system of dogs in vivo. A mechanism for regulated insulin delivery to the brain. J Clin Invest. 92:1824–1830.

Beattie EC, Carroll RC, Yu X, Morishita W, Yasuda H, von Zastrow M, Malenka RC. 2000. Regulation of AMPA receptor endocytosis by a signaling mechanism shared with LTD. Nat Neurosci. 3:1291–1300.

Biessels GJ, Kamal A, Ramakers GM, Urban IJ, Spruijt BM, Erkelens DW, Gispen WH. 1996. Place learning and hippocampal synaptic plasticity in streptozotocin-induced diabetic rats. Diabetes. 45:1259–1266.

Bliss TV, Collingridge GL. 1993. A synaptic model of memory: long-term potentiation in the hippocampus. Nature. 361:31–39.

Burks DJ, Font de Mora J, Schubert M, Withers DJ, Myers MG, Towery HH, Altamuro SL, Flint CL, White MF. 2000. IRS-2 pathways integrate female reproduction and energy homeostasis. Nature. 407:377–382.

Chiu SL, Chen CM, Cline HT. 2008. Insulin receptor signaling regulates synapse number, dendritic plasticity, and circuit function in vivo. Neuron. 58:708–719.

Choudhury AI, Heffron H, Smith MA, Al-Qassab H, Xu AW, Selman C, Simmgen M, Clements M, Claret M, Maccoll G, et al. 2005. The role of insulin receptor substrate 2 in hypothalamic and beta cell function. J Clin Invest. 115:940–950.

Clarke DW, Mudd L, Boyd FT, Jr., Fields M, Raizada MK. 1986. Insulin is released from rat brain neuronal cells in culture. J Neurochem. 47:831–836.

Collingridge GL, Kehl SJ, McLennan H. 1983. Excitatory amino acids in synaptic transmission in the Schaffer collateral-commissural pathway of the rat hippocampus. J Physiol. 334:33–46.

Craft S. 2007. Insulin resistance and Alzheimer's disease pathogenesis: potential mechanisms and implications for treatment. Curr Alzheimer Res. 4:147–152.

Davidson D, Viallet J, Veillette A. 1994. Unique catalytic properties dictate the enhanced function of p59fynT, the hemopoietic cell-specific isoform of the Fyn tyrosine protein kinase, in T cells. Mol Cell Biol. 14:4554–4564.

Desrocher M, Rovet J. 2004. Neurocognitive correlates of type 1 diabetes mellitus in childhood. Child Neuropsychol. 10:36–52.

Dou JT, Chen M, Dufour F, Alkon DL, Zhao WQ. 2005. Insulin receptor signaling in long-term memory consolidation following spatial learning. Learn Mem. 12:646–655.

Elias MF, Elias PK, Sullivan LM, Wolf PA, D'Agostino RB. 2003. Lower cognitive function in the presence of obesity and hypertension: the Framingham heart study. Int J Obes Relat Metab Disord. 27:260–268.

English JD, Sweatt JD. 1996. Activation of p42 mitogen-activated protein kinase in hippocampal long term potentiation. J Biol Chem. 271:24329–24332.

Feng W, Zhang M. 2009. Organization and dynamics of PDZ-domain-related supramodules in the postsynaptic density. Nat Rev Neurosci. 10:87–99.

Folli F, Bonfanti L, Renard E, Kahn CR, Merighi A. 1994. Insulin receptor substrate-1 (IRS-1) distribution in the rat central nervous system. J Neurosci. 14:6412–6422.

Garcia-Estrada J, Garcia-Segura LM, Torres-Aleman I. 1992. Expression of insulin-like growth factor I by astrocytes in response to injury. Brain Res. 592:343–347.

Garcia-Segura LM, Perez J, Pons S, Rejas MT, Torres-Aleman I. 1991. Localization of insulin-like growth factor I (IGF-I)-like immunoreactivity in the developing and adult rat brain. Brain Res. 560:167–174.

Grant SG, O'Dell TJ, Karl KA, Stein PL, Soriano P, Kandel ER. 1992. Impaired long-term potentiation, spatial learning, and hippocampal development in fyn mutant mice. Science. 258:1903–1910.

Gunton JE, Kulkarni RN, Yim S, Okada T, Hawthorne WJ, Tseng YH, Roberson RS, Ricordi C, O'Connell PJ, Gonzalez FJ, et al. 2005. Loss of ARNT/HIF1beta mediates altered gene expression and pancreatic-islet dysfunction in human type 2 diabetes. Cell. 122:337–349.

Hestrin S, Nicoll RA, Perkel DJ, Sah P. 1990. Analysis of excitatory synaptic action in pyramidal cells using whole-cell recording from rat hippocampal slices. J Physiol. 422:203–225.

Imaeda A, Kaneko T, Aoki T, Kondo Y, Nagase H. 2002. DNA damage and the effect of antioxidants in streptozotocin-treated mice. Food Chem Toxicol. 40:979–987.

Kamal A, Biessels GJ, Gispen WH, Ramakers GM. 2006. Synaptic transmission changes in the pyramidal cells of the hippocampus in streptozotocin-induced diabetes mellitus in rats. Brain Res. 1073–1074:276–280.

Kanterewicz BI, Urban NN, McMahon DB, Norman ED, Giffen LJ, Favata MF, Scherle PA, Trzskos JM, Barrionuevo G, Klann E. 2000. The extracellular signal-regulated kinase cascade is required for NMDA receptor-independent LTP in area CA1 but not area CA3 of the hippocampus. J Neurosci. 20:3057–3066.

Kern W, Peters A, Fruehwald-Schultes B, Deininger E, Born J, Fehm HL. 2001. Improving influence of insulin on cognitive functions in humans. Neuroendocrinology. 74:270–280.

Kubota N, Terauchi Y, Tobe K, Yano W, Suzuki R, Ueki K, Takamoto I, Satoh H, Maki T, Kubota T, et al. 2004. Insulin receptor substrate 2 plays a crucial role in beta cells and the hypothalamus. J Clin Invest. 114:917–927.

Kullmann DM. 1994. Amplitude fluctuations of dual-component EPSCs in hippocampal pyramidal cells: implications for long-term potentiation. Neuron. 12:1111–1120.

Kuusisto J, Koivisto K, Mykkanen L, Helkala EL, Vanhanen M, Hanninen T, Kervinen K, Kesaniemi YA, Riekkinen PJ, Laakso M. 1997. Association between features of the insulin resistance syndrome and Alzheimer's disease independently of apolipoprotein E4 phenotype: cross sectional population based study. BMJ. 315:1045–1049.

Lin JW, Ju W, Foster K, Lee SH, Ahmadian G, Wyszynski M, Wang YT, Sheng M. 2000. Distinct molecular mechanisms and divergent endocytotic pathways of AMPA receptor internalization. Nat Neurosci. 3:1282–1290.

Liu L, Brown JC, 3rd, Webster WW, Morrisett RA, Monaghan DT. 1995. Insulin potentiates N-methyl-D-aspartate receptor activity in Xenopus oocytes and rat hippocampus. Neurosci Lett. 192:5–8.

Liu SC, Wang Q, Lienhard GE, Keller SR. 1999. Insulin receptor substrate 3 is not essential for growth or glucose homeostasis. J Biol Chem. 274:18093–18099.

Luchsinger JA, Tang MX, Shea S, Mayeux R. 2004. Hyperinsulinemia and risk of Alzheimer disease. Neurology. 63:1187–1192.

Malenka RC, Nicoll RA. 1999. Long-term potentiation—a decade of progress? Science. 285:1870–1874.

Man HY, Wang Q, Lu WY, Ju W, Ahmadian G, Liu L, D'Souza S, Wong TP, Taghibiglou C, Lu J, et al. 2003. Activation of PI3-kinase is required for AMPA receptor insertion during LTP of mEPSCs in cultured hippocampal neurons. Neuron. 38:611–624.

Martin ED, Buno W. 2003. Caffeine-mediated presynaptic long-term potentiation in hippocampal CA1 pyramidal neurons. J Neurophysiol. 89:3029–3038.

Martin ED, Pozo MA. 2004. Valproate reduced excitatory postsynaptic currents in hippocampal CA1 pyramidal neurons. Neuropharmacology. 46:555–561.

Mastick CC, Saltiel AR. 1997. Insulin-stimulated tyrosine phosphorylation of caveolin is specific for the differentiated adipocyte phenotype in 3T3-L1 cells. J Biol Chem. 272:20706–20714.

Messier C. 2005. Impact of impaired glucose tolerance and type 2 diabetes on cognitive aging. Neurobiol Aging. 26(Suppl 1):26–30.

Moloney AM, Griffin RJ, Timmons S, O'Connor R, Ravid R, O'Neill C. 2010. Defects in IGF-1 receptor, insulin receptor and IRS-1/2 in Alzheimer's disease indicate possible resistance to IGF-1 and insulin signalling. Neurobiol Aging. 31:224–243

Myers MG, Jr., Backer JM, Sun XJ, Shoelson S, Hu P, Schlessinger J, Yoakim M, Schaffhausen B, White MF. 1992. IRS-1 activates phosphatidylinositol 3′-kinase by associating with src homology 2 domains of p85. Proc Natl Acad Sci U S A. 89:10350–10354.

Nicoll RA, Malenka RC. 1999. Expression mechanisms underlying NMDA receptor-dependent long-term potentiation. Ann N Y Acad Sci. 868:515–525.

Nishijima T, Piriz J, Duflot S, Fernandez AM, Gaitan G, Gomez-Pinedo U, Verdugo JM, Leroy F, Soya H, Nuñez A, et al. 2010. Neuronal activity drives localized blood-brain-barrier transport of serum insulin-like growth factor-I into the CNS. Neuron. 67:834–846.

Peineau S, Taghibiglou C, Bradley C, Wong TP, Liu L, Lu J, Lo E, Wu D, Saule E, Bouschet T, et al. 2007. LTP inhibits LTD in the hippocampus via regulation of GSK3beta. Neuron. 53:703–717.

Poncer JC, Malinow R. 2001. Postsynaptic conversion of silent synapses during LTP affects synaptic gain and transmission dynamics. Nat Neurosci. 4:989–996.

Pons S, Rejas MT, Torres-Aleman I. 1991. Ontogeny of insulin-like growth factor I, its receptor, and its binding proteins in the rat hypothalamus. Brain Res Dev Brain Res. 62:169–175.

Raizada MK, Shemer J, Judkins JH, Clarke DW, Masters BA, LeRoith D. 1988. Insulin receptors in the brain: structural and physiological characterization. Neurochem Res. 13:297–303.

Reger MA, Watson GS, Green PS, Wilkinson CW, Baker LD, Cholerton B, Fishel MA, Plymate SR, Breitner JC, DeGroodt W, et al. 2008. Intranasal insulin improves cognition and modulates beta-amyloid in early AD. Neurology. 70:440–448.

Rivera E, Ajani JA. 1998. Doxorubicin, streptozocin, and 5-fluorouracil chemotherapy for patients with metastatic islet-cell carcinoma. Am J Clin Oncol. 21:36–38.

Rivera EJ, Goldin A, Fulmer N, Tavares R, Wands JR, de la Monte SM. 2005. Insulin and insulin-like growth factor expression and function deteriorate with progression of Alzheimer's disease: link to brain reductions in acetylcholine. J Alzheimers Dis. 8:247–268.

Ronnemaa E, Zethelius B, Sundelof J, Sundstrom J, Degerman-Gunnarsson M, Berne C, Lannfelt L, Kilander L. 2008. Impaired insulin secretion increases the risk of Alzheimer disease. Neurology. 71:1065–1071.

Rostas JA, Brent VA, Voss K, Errington ML, Bliss TV, Gurd JW. 1996. Enhanced tyrosine phosphorylation of the 2B subunit of the N-methyl-D-aspartate receptor in long-term potentiation. Proc Natl Acad Sci U S A. 93:10452–10456.

Saal D, Dong Y, Bonci A, Malenka RC. 2003. Drugs of abuse and stress trigger a common synaptic adaptation in dopamine neurons. Neuron. 37:577–582.

Schlessinger J, Mohammadi M, Margolis B, Ullrich A. 1992. Role of SH2-containing proteins in cellular signaling by receptor tyrosine kinases. Cold Spring Harb Symp Quant Biol. 57:67–74.

Schubert M, Brazil DP, Burks DJ, Kushner JA, Ye J, Flint CL, Farhang-Fallah J, Dikkes P, Warot XM, Rio C, et al. 2003. Insulin receptor substrate-2 deficiency impairs brain growth and promotes tau phosphorylation. J Neurosci. 23:7084–7092.

Selman C, Lingard S, Choudhury AI, Batterham RL, Claret M, Clements M, Ramadani F, Okkenhaug K, Schuster E, Blanc E, et al. 2008. Evidence for lifespan extension and delayed age-related biomarkers in insulin receptor substrate 1 null mice. FASEB J. 22:807–818.

Shalin SC, Hernandez CM, Dougherty MK, Morrison DK, Sweatt JD. 2006. Kinase suppressor of Ras1 compartmentalizes hippocampal signal transduction and subserves synaptic plasticity and memory formation. Neuron. 50:765–779.

Sheng M. 2001. The postsynaptic NMDA-receptor—PSD-95 signaling complex in excitatory synapses of the brain. J Cell Sci. 114:1251.

Skeberdis VA, Lan J, Zheng X, Zukin RS, Bennett MV. 2001. Insulin promotes rapid delivery of N-methyl-D-aspartate receptors to the cell surface by exocytosis. Proc Natl Acad Sci U S A. 98:3561–3566.

Stranahan AM, Arumugam TV, Cutler RG, Lee K, Egan JM, Mattson MP. 2008. Diabetes impairs hippocampal function through glucocorticoid-mediated effects on new and mature neurons. Nat Neurosci. 11:309–317.

Sun XJ, Pons S, Asano T, Myers MG, Jr., Glasheen E, White MF. 1996. The Fyn tyrosine kinase binds Irs-1 and forms a distinct signaling complex during insulin stimulation. J Biol Chem. 271:10583–10587.

Sun XJ, Rothenberg P, Kahn CR, Backer JM, Araki E, Wilden PA, Cahill DA, Goldstein BJ, White MF. 1991. Structure of the insulin receptor substrate IRS-1 defines a unique signal transduction protein. Nature. 352:73–77.

Unger J, McNeill TH, Moxley RT, 3rd, White M, Moss A, Livingston JN. 1989. Distribution of insulin receptor-like immunoreactivity in the rat forebrain. Neuroscience. 31:143–157.
van der Heide LP, Kamal A, Artola A, Gispen WH, Ramakers GM. 2005. Insulin modulates hippocampal activity-dependent synaptic plasticity in a N-methyl-d-aspartate receptor and phosphatidyl-inositol-3-kinase-dependent manner. J Neurochem. 94:1158–1166.
Vanhanen M, Koivisto K, Moilanen L, Helkala EL, Hanninen T, Soininen H, Kervinen K, Kesaniemi YA, Laakso M, Kuusisto J. 2006. Association of metabolic syndrome with Alzheimer disease: a population-based study. Neurology. 67:843–847.
Vetiska SM, Ahmadian G, Ju W, Liu L, Wymann MP, Wang YT. 2007. GABAA receptor-associated phosphoinositide 3-kinase is required for insulin-induced recruitment of postsynaptic GABAA receptors. Neuropharmacology. 52:146–155.
Villasana LE, Klann E, Tejada-Simon MV. 2006. Rapid isolation of synaptoneurosomes and postsynaptic densities from adult mouse hippocampus. J Neurosci Methods. 158:30–36.
Wan Q, Xiong ZG, Man HY, Ackerley CA, Braunton J, Lu WY, Becker LE, MacDonald JF, Wang YT. 1997. Recruitment of functional GABA(A) receptors to postsynaptic domains by insulin. Nature. 388:686–690.
Wang Q, Liu L, Pei L, Ju W, Ahmadian G, Lu J, Wang Y, Liu F, Wang YT. 2003. Control of synaptic strength, a novel function of Akt. Neuron. 38:915–928.
White MF. 1997. The insulin signalling system and the IRS proteins. Diabetologia. 40(Suppl 2):S2–S17.
Whitmer RA, Gunderson EP, Barrett-Connor E, Quesenberry CP, Jr., Yaffe K. 2005. Obesity in middle age and future risk of dementia: a 27 year longitudinal population based study. BMJ. 330:1360.
Winder DG, Martin KC, Muzzio IA, Rohrer D, Chruscinski A, Kobilka B, Kandel ER. 1999. ERK plays a regulatory role in induction of LTP by theta frequency stimulation and its modulation by beta-adrenergic receptors. Neuron. 24:715–726.
Withers DJ, Burks DJ, Towery HH, Altamuro SL, Flint CL, White MF. 1999. Irs-2 coordinates Igf-1 receptor-mediated beta-cell development and peripheral insulin signalling. Nat Genet. 23:32–40.
Withers DJ, Gutierrez JS, Towery H, Burks DJ, Ren JM, Previs S, Zhang Y, Bernal D, Pons S, Shulman GI, et al. 1998. Disruption of IRS-2 causes type 2 diabetes in mice. Nature. 391:900–904.
Xu F, Plummer MR, Len GW, Nakazawa T, Yamamoto T, Black IB, Wu K. 2006. Brain-derived neurotrophic factor rapidly increases NMDA receptor channel activity through Fyn-mediated phosphorylation. Brain Res. 1121:22–34.
Yamato T, Misumi Y, Yamasaki S, Kino M, Aomine M. 2004. Diabetes mellitus decreases hippocampal release of neurotransmitters: an in vivo microdialysis study of awake, freely moving rats. Diabetes Nutr Metab. 17:128–136.
Ye P, Li L, Lund PK, D'Ercole AJ. 2002. Deficient expression of insulin receptor substrate-1 (IRS-1) fails to block insulin-like growth factor-I (IGF-I) stimulation of brain growth and myelination. Brain Res Dev Brain Res. 136:111–121.
Yu XM, Askalan R, Keil GJ, Salter MW. 1997. NMDA channel regulation by channel-associated protein tyrosine kinase Src. Science. 275:674–678.
Zhao W, Chen H, Xu H, Moore E, Meiri N, Quon MJ, Alkon DL. 1999. Brain insulin receptors and spatial memory. Correlated changes in gene expression, tyrosine phosphorylation, and signaling molecules in the hippocampus of water maze trained rats. J Biol Chem. 274:34893–34902.
Zucker RS. 1989. Short-term synaptic plasticity. Annu Rev Neurosci. 12:13–31.